Correlating the magic numbers of inorganic nanomolecular assemblies with a $\{Pd_{84}\}$ molecular-ring Rosetta Stone

Feng Xu, Haralampos N. Miras, Rachel A. Scullion, De-Liang Long, Johannes Thiel, and Leroy Cronin[1]

WestCHEM, School of Chemistry, University of Glasgow, Joseph Black Building, University Avenue, Glasgow G12 8QQ, United Kingdom

Edited by* Malcolm H. Chisholm, The Ohio State University, Columbus, OH, and approved June 7, 2012 (received for review February 21, 2012)

Molecular self-assembly has often been suggested as the ultimate route for the bottom-up construction of building blocks atom-by-atom for functional nanotechnology, yet structural design or prediction of nanomolecular assemblies is still far from reach. Whereas nature uses complex machinery such as the ribosome, chemists use painstakingly engineered step-by-step approaches to build complex molecules but the size and complexity of such molecules, not to mention the accessible yields, can be limited. Herein we present the discovery of a palladium oxometalate $\{Pd_{84}\}$-ring cluster 3.3 nm in diameter; $[Pd_{84}O_{42}(OAc)_{28}(PO_4)_{42}]^{70-}$ ($\{Pd_{84}\} \equiv \{Pd_{12}\}_7$) that is formed in water just by mixing two reagents at room temperature, giving crystals of the compound in just a few days. The structure of the $\{Pd_{84}\}$-ring has sevenfold symmetry, comprises 196 building blocks, and we also show, using mass spectrometry, that a large library of other related nanostructures is present in solution. Finally, by analysis of the symmetry and the building block library that construct the $\{Pd_{84}\}$ we show that the correlation of the symmetry, subunit number, and overall cluster nuclearity can be used as a "Rosetta Stone" to rationalize the "magic numbers" defining a number of other systems. This is because the discovery of $\{Pd_{84}\}$ allows the relationship between seemingly unrelated families of molecular inorganic nanosystems to be decoded from the overall cluster magic-number nuclearity, to the symmetry and building blocks that define such structures allowing the prediction of other members of these nanocluster families.

polyoxopalladates | {M84} cluster | noble metals | inorganic chemistry | self assembly

Functional nanotechnology requires control of nanomolecular architectures (1–3) that probably can only be achieved by self-assembly from the bottom up (4, 5) but this process itself is very difficult to predict, rationalize, or control. In self-assembly, the observation of symmetrically favored numbers of metal nuclearity ("magic numbers") (6) or shapes with high symmetry, such as icosahedra (7) and rings (8–10), may provide a theoretical basis for the reliable and controlled fabrication of complex molecular architectures. In this respect we hypothesized that it is important to design minimal systems that use only a small number of chemical components, but with a vast library of possible architectures, and to use the techniques of structural and analytical chemistry to probe the range of accessible molecular architectures. By conducting such solution studies, combined with structural analysis, our aim has been to understand the overall cluster nuclearity and structure to reveal the underlying principles that link symmetry to structure with the overall grand aim of the a priori design of molecular nanosystems from the bottom up using self-assembly.

Here, we present the discovery of a complex self-assembled system in which the architectural beauty and molecular complexity are orchestrated by symmetry and a library of dynamic subunits, and this is achieved by mixing only two components in water: Palladium(II) acetate and phosphate buffer. We choose Pd(II) in this study for two main reasons: Firstly, it has a well-known controllable and spontaneous behavior in metal-directed assembly, such as molecular capsules, due to its smaller coordination number and greater preference for square-planar geometry than other transition metal ions (11, 12); and secondly the recent discovery of polyoxopalladates (13, 14). In 2011 we reported a $\{\mathbf{Pd_{17}}\}$ cluster compound, $Na_6[H_9Pd_{17}O_{10}(PO_4)_{10}]$, which is formed by heating a system of $Pd_3(OAc)_6$ in NaH_2PO_4-Na_2HPO_4 solution for 90 min (14). In this reaction, a library of at least three different building units can be defined: quadrangular $\{Pd_4O_4\}$ and pentagonal $\{Pd_5O_5\}$ moieties that can be easily recognized, but the existence of eight tetrahedral $\{Pd_4\}$ subunits with eight rare interstitial oxo ligands is also observed (15, 16). We found this structure important because it contained highly condensed $\{Pd_4(\mu_4\text{-}O)\}$ units that we imagined could be very versatile building blocks (17). To explore the potential of these building blocks to link in different ways, we set out to explore similar reactions under a series of different reaction conditions by changing temperature, pH, and crystallization methods. When the reaction was carried out at room temperature, a vast envelope of very high nuclearity and charged protein-sized inorganic molecules was revealed in the m/z range of 10–25 kD by electrospray mass spectrometry experiments. This was in stark contrast to the higher temperature experiments that showed no such envelope; see Fig. 1. Although the complexity of the envelope did not allow the unambiguous assignment of the species present, it was evident that a number of very large molecules were formed from a very simple two-component reaction with a large range of possible charges (Fig. 1). Upon standing of the solution for a few days, a gigantic >16 kD nanomolecular architecture was crystallized from this mixture as a ring-shaped $\{\mathbf{Pd_{84}}\}$ of the formula $[Pd_{84}O_{42}(OAc)_{28}(PO_4)_{42}]^{70-}$ in up to 20% yield; the ring has an outer and inner diameter of 3.3 nm and 1 nm, respectively. What is most remarkable is that the synthesis is almost identical to that of the much smaller $\{\mathbf{Pd_{17}}\}$, where the only difference was that the reaction solution temperature was strictly controlled at 25 °C, and the observation of the vast library of species from the room temperature reactions reinforces the importance of reaction temperature. Furthermore, there appeared to be an interesting coincidence whereby the largest Mn-based nanostructure is also a $\{\mathbf{Mn_{84}}\}$ wheel but with completely different building blocks (8).

Results and Discussion

Structural Analysis of $\{Pd_{84}\}$. The $\{\mathbf{Pd_{84}}\}$ cluster is significantly larger than any polyoxopalladate seen hitherto, and shows that

---

Author contributions: L.C. designed research; F.X. and R.A.S. performed research; H.N.M., D.L., and J.T. contributed new reagents/analytic tools; F.X., H.N.M., D.L., J.T., and L.C. analyzed data; and F.X. and L.C. wrote the paper.

The authors declare no conflict of interest.

*This Direct Submission article had a prearranged editor.

Data deposition: The atomic coordinates have been deposited in the Cambridge Structural Database, Cambridge Crystallographic Data Centre, Cambridge CB2 1EZ, United Kingdom (CSD reference no. 846615).

[1] To whom correspondence should be addressed. E-mail: lee.cronin@glasgow.ac.uk.

This article contains supporting information online at www.pnas.org/lookup/suppl/doi:10.1073/pnas.1202981109/-/DCSupplemental.

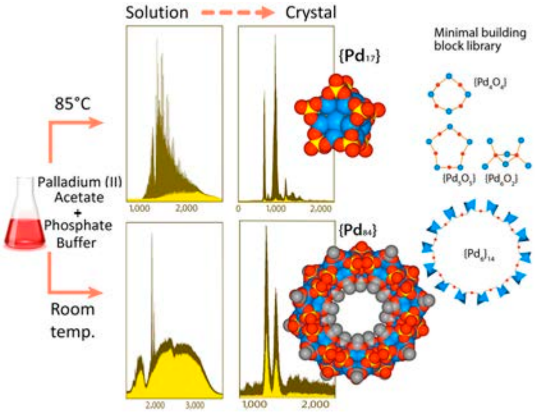

Fig. 1. Reaction scheme showing the conditions for the assembly of $\{\mathbf{Pd_{17}}\}$ and $\{\mathbf{Pd_{84}}\}$, their resulting structures, and the building blocks present in each cluster. The mass spectra of the reaction mixtures for each cluster are shown on the *Left*, which shows the very large number of very high mass species in the room temperature reaction (*Bottom*, *Left*) vs. the high temperature reaction (*Top*, *Left*), as well as those of the pure compounds on the *Right*. The crystal structures of $\{\mathbf{Pd_{17}}\}$ and $\{\mathbf{Pd_{84}}\}$ are shown as space-filling models: Pd, blue; O, red; P, yellow; C, gray. On the far *Right*, a depiction of the minimal building block library found in the $\{\mathbf{Pd_{17}}\}$ is represented showing the variety of available architectures. Notably $\{Pd_6O_2\}$, found in the $\{\mathbf{Pd_{17}}\}$, is the key building block that is linked into the wheel and this connected framework is shown on the right. The blue "butterfly" polyhedra represents the $\{Pd_6O_2\}$ units.

gigantic ring architectures hold a special position in inorganic "supermolecular" chemistry. The $\{\mathbf{Pd_{84}}\}$ ring has D_{7d} symmetry containing a C_7 (S_{14}) axis (Fig. 2) and the cluster can be decomposed into seven $\{[Pd_6(\mu_4\text{-}O)_2(\mu_2\text{-}O)(OAc)_2(PO_4)_3]_2\} \equiv \{\mathbf{Pd_6}\}_2$ or $\{\mathbf{Pd_{12}}\}$ subunits, allowing us to suggest that $\{\mathbf{Pd_6}\}$ could be the "minimal" structural repeating unit that is dimerized to the formal $\{\mathbf{Pd_{12}}\}$ building block. In the $\{\mathbf{Pd_6}\}$ minimal building unit, six palladium atoms are linked together by two unusual μ_4-O ligands (15, 16). This interstitial μ_4-O unit templates each of the two linked tetrahedra in the form of $\{\mu_4\text{-}O\text{-}Pd_4\}$ that share a Pd-Pd edge. The distance between the edge-sharing palladium ions is 2.92 Å, whereas the other Pd-Pd distances within the subunit are longer and lie between 3.20 Å and 3.51 Å.

Each of the resulting $\{\mathbf{Pd_6}\}$ subunits is capped by two phosphate ligands, which are positioned outside the core of $\{\mathbf{Pd_6}\}$. Furthermore, the 14 $\{\mathbf{Pd_6}\}$ subunits in the wheel are directly linked together by μ_2-O ligands. Four acetate and two phosphate ligands bridge adjacent $\{\mathbf{Pd_6}\}$ units in μ_2- and μ_4-coordination modes, respectively (Fig. 2 and *SI Appendix*, Fig. S1). It is interesting to note that one of the acetate ligands in each of the 14 $\{\mathbf{Pd_6}\}$ subunits is pointing towards the inside of the cavity of the $\{\mathbf{Pd_{84}}\}$ ring, whereas the other one adopts an up/down direction alternatively towards the outside, and this allows the acetate ligands in adjacent $\{\mathbf{Pd_6}\}$ to be staggered presumably minimizing steric interactions. Additionally, the periphery of the nanosized ring is populated by phosphate ligands whereas the interior rim of the wheel is populated by methyl-groups of the acetate ligands that point inwards, thus defining hydrophilic and hydrophobic domains, respectively. Therefore, the cluster anion of $\{\mathbf{Pd_{84}}\}$ can be formulated as a tetradecamer of $\{\mathbf{Pd_6}\}$ units, building up to $\{\mathbf{Pd_6}\}_{\mathbf{14}} \equiv \{Pd_6(\mu_4\text{-}O)_2(\mu_2\text{-}O)(OAc)_2(PO_4)_3\}_{14}$ in 14-fold symmetric system (Figs. 1 and 2).

Linking the Magic Number and the Building Block Principle of the $\{\mathbf{Pd_{84}}\}$ Ring with Other Macromolecular Inorganic Systems. One of the most important consequences of this work is that the $\{\mathbf{Pd_{84}}\}$ ring-cluster reveals the possibility of generating a supermolecular wheel structure from late transition metals through a very simple "one-pot" two-component reaction. Although the family of known molecular wheels is large, many of them incorporate less than 32 metal ions. The only exceptions to this include $\{\mathbf{Mn_{84}}\}$ reported by Christou et al. (13), and the giant $\{\mathbf{Mo_{154}}\}$ reported by Müller et al. (10), which are built up by early transition metal ions. The similarity between the $\{\mathbf{Pd_{84}}\}$ and $\{\mathbf{Mn_{84}}\}$ wheel in terms of nuclearity is remarkable, especially given the radically different subunit composition. From analysis of the $\{\mathbf{Pd_{84}}\}$ we are able to show that the symmetry-building block correlation of $\{\mathbf{Pd_{84}}\}$ with the other known families of clusters, e.g., $\{\mathbf{Mo_x}\}$ and $\{\mathbf{Mn_x}\}$ allows us to present a "Rosetta Stone" framework to decode these other families of molecular nanoclusters. The possibility of such magic numbers is important as they show a connection between the architectural principles that define the clusters; see Fig. 3. These would be defined by symmetry and building blocks in highly symmetrical structures and can be expressed in the form of specific shapes and patterns in self-assembly. For instance, despite the same nuclearity as $\{\mathbf{Pd_{84}}\}$, the $\{\mathbf{Mn_{84}}\}$ cluster has the more common sixfold symmetry with a roughly D_{6d} point group and a C_6 (S_{12}) axis (methyl groups on methanol ligands are not counted) with six $\{\mathbf{Mn_{14}}\}$ repeating units, and the $\{\mathbf{Mo_{154}}\}$ also has the same symmetry as the $\{\mathbf{Pd_{84}}\}$ but the building block nuclearity in each cluster is 22 and 12 [for symmetry seven (C_7) but could also be expressed equivalently with building block numbers 11 and 6 for symmetry 14 (S_{14})], respectively ($22 \times 7 = 154$; $12 \times 7 = 84$). Not only is 84 a magic common number as seen here in $\{\mathbf{Pd_{84}}\}$ and $\{\mathbf{Mn_{84}}\}$ structures (and also link to the $\{\mathbf{Mo_{154}}\}$), but observations made in the structures of $\{\mathbf{Mn_{84}}\}$, $\{\mathbf{Pd_{84}}\}$, and $\{\mathbf{Mo_{154}}\}$ constitute a new minimal language that could lead to a universal instruction set in the assembly of gigantic nanomolecular architectures. It would also appear that this can even be extended from wheel structures to ball-shaped

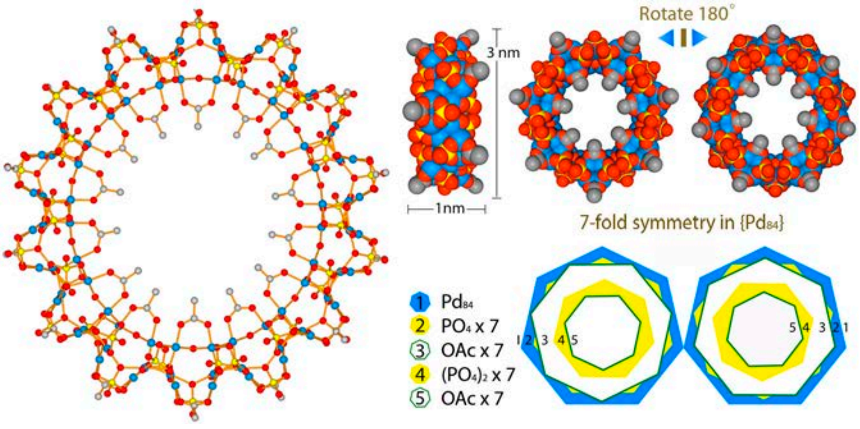

Fig. 2. *Left* A ball and stick representation of the $\{\mathbf{Pd_{84}}\}$ cluster. *Top*, *Right* A space filling model, side, plane, and rotated plane of $\{\mathbf{Pd_{84}}\}$. *Bottom*, *Right*: A description of the sevenfold rotational symmetry associated with the $\{\mathbf{Pd_{84}}\}$. Color scheme; Pd—blue, O—red, P—yellow, C—gray.

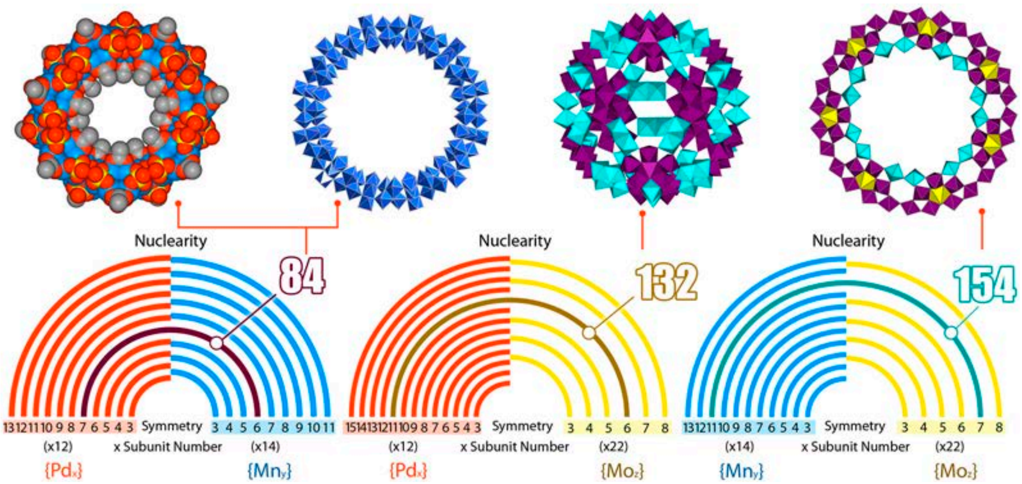

Fig. 3. *Top* Representations of a space filling model of the $\{\mathbf{Pd_{84}}\}$ cluster, a polyhedral representation of $\{\mathbf{Mn_{84}}\}$, and polyhedral representations of $\{\mathbf{Mo_{132}}\}$ and $\{\mathbf{Mo_{154}}\}$. *Bottom* Symmetry—subunit correlation diagrams indicating Pd-Mn, Pd-Mo, and Mn-Mo showing possible interesting nuclearities correlated at 84 for Mn and Pd, 132 for Pd and Mo, and 154 for Mn-Mo showing the correspondence between the cluster families.

super fullerenes (18); see Fig. 3. This means this approach could lead to the rationalization of the overall cluster nuclearity (N), or magic number, as a function of the symmetry number (S) and building-block nuclearity (n) according to $n \times S = N$; for example, for $\{\mathbf{Pd_{84}}\}$, sevenfold symmetric with $\{\mathbf{Pd_{12}}\}$ building blocks: $7 \times 12 = 84$; for $\{\mathbf{Mn_{84}}\}$, sixfold symmetric with $\{\mathbf{Mn_{14}}\}$ building blocks: $6 \times 14 = 84$; for $\{\mathbf{Mo_{154}}\}$, sevenfold symmetric with $\{\mathbf{Mo_{22}}\}$ building blocks: $7 \times 22 = 154$.

Based on our discussion above, we now have a general approach that can be applied in any system that is governed by self-assembly processes, such as Pd-oxometalates, Mo-blues, and Mn-clusters as particular examples, but this should have general applicability to any self-assembled system. This is because, based on the symmetry of the isolated compound and the number of building units used for its assembly, there is a long list of self-assembled materials that can be theoretically synthesized and exhibit different nuclearities. The long list of different nuclearities belongs to an arithmetic sequence that can be described by the general formula $N_m = n(S+1)$ where N_m defines the next magic number member in the series of symmetry numbers $(S+1)$, and n is the nuclearity of the "repeating" building blocks. From this extended map of nuclearities, a large majority will be excluded based on the restrictions introduced by the symmetry and by restrictions imposed by the available building block library, which exist for each chemical system and have been already observed experimentally from crystallographic investigations. Given these observations we are able to predict some new members of the $\{\mathbf{Mo_x}\}$, $\{\mathbf{Mn_x}\}$, and $\{\mathbf{Pd_x}\}$ simply based upon the observed building block libraries and available symmetries. For the Mn system it would seem feasible that the $\{\mathbf{Mn_{70}}\}$ (14×5) and $\{\mathbf{Mn_{98}}\}$ (14×7) are possible, and for the Mo system that $\{\mathbf{Mo_{110}}\}$ (22×5) is possible. Note that the $\{\mathbf{Mo_{132}}\}$ (22×6) and $\{\mathbf{Mo_{176}}\}$ (22×8) have already been observed in addition to the archetypal $\{\mathbf{Mo_{154}}\}$ (22×7) nanowheels first revealed by Müller et al. in 1995 (10) as has the gigantic ball-wheel hybrid $\{\mathbf{Mo_{368}}\}$ (23×16) (3). This means that access to the 11-fold symmetric $\{\mathbf{Pd_x}\}$ and $\{\mathbf{Mn_x}\}$ clusters would yield $\{\mathbf{Pd_{132}}\}$ and $\{\mathbf{Mn_{154}}\}$ clusters, respectively; however, such symmetries are difficult to imagine. By using the same arguments we predict that the assembly and isolation of the $\{\mathbf{Pd_{60}}\}$ (12×5), $\{\mathbf{Pd_{72}}\}$ (12×6), and $\{\mathbf{Pd_{96}}\}$ (12×8) but also it is worth noting that the $\{\mathbf{Pd_{60}}\}$ could also be accessed by other symmetries making the structure of this appealing magic number even more likely. It is interesting to note, in terms of predictions, the existence of the $\{\mathbf{Mn_{70}}\}$ has been experimentally revealed, although the structure has not been formally published (19). Although we present a single new $\{\mathbf{Pd_{84}}\}$ structure here, this theoretical framework connects three previously unconnected cluster families (with nuclearities >60) with eight cluster types: $\{\mathbf{Mn_{70}}\}$, $\{\mathbf{Mn_{84}}\}$, $\{\mathbf{Pd_{84}}\}$, $\{\mathbf{Mo_{102}}\}$, $\{\mathbf{Mo_{132}}\}$, $\{\mathbf{Mo_{154}}\}$, $\{\mathbf{Mo_{176}}\}$, and $\{\mathbf{Mo_{368}}\}$, providing validation of this framework. Further, if we extend this analysis to lower nuclearity frameworks then this approach also works but the symmetries of the clusters need to be idealized.

Solution Studies of the Two-Component Reaction. From our solution measurements from the mother liquor of the $\{\mathbf{Pd_{84}}\}$ system, it is clear that there is an incredibly large number of other clusters species in solution; see Fig. 4. Not only do species populate the m/z range of 1,250–3,450, but possible charge states for the species range from −7 to −9 giving a mass range of 10–25 kD. This means that a large variety of hitherto structurally undiscovered $\{\mathbf{Pd_x}\}$ are possible. The $\{\mathbf{Pd_{60}}\}$ and $\{\mathbf{Pd_{72}}\}$ prediction is especially informative and tantalizing because $\{\mathbf{Pd_{12}}\}_\mathbf{x}$ ($x = 5$ or 6), by the oligomerization of the virtual building block $\{\mathbf{Pd_{12}}\}$, should be allowed. This proposal is supported by our crystallographic observation of $\{\mathbf{Pd_{84}}\} \equiv \{\mathbf{Pd_{12}}\}_\mathbf{x}$, ($x = 7$) and is consistent with our

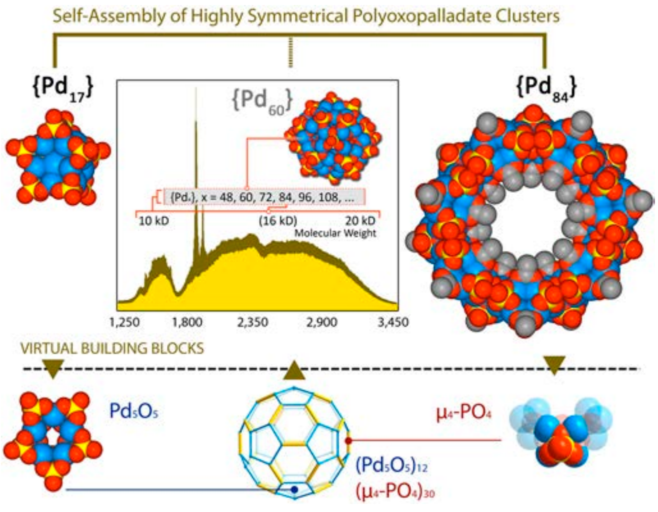

Fig. 4. Scheme showing $\{\mathbf{Pd_{17}}\}$ and $\{\mathbf{Pd_{84}}\}$ along with $\{Pd_5O_5\}$ and $\{\mu_4\text{-}PO_4\}$ units found in each cluster, respectively. Importantly the here predicted $\{\mathbf{Pd_{60}}\}$ cluster contains both these building units and is a high probability structure according to the analysis presented and the solution mass spectrum that contains peak envelopes consistent with those expected for predicted clusters (by formula analysis) is shown.

preliminary mass spectrometry studies. Furthermore, the $\{\mathbf{Pd}_{17}\}$ not only contains the $\{\mathbf{Pd}_{6}\}$ building block found in the $\{\mathbf{Pd}_{84}\}$ but also a $\{\mathbf{Pd}_{5}\}$ building block that could offer another route to assemble the $\{\mathbf{Pd}_{60}\}$ (see Movie S1).

Conclusions

In summary we have presented the discovery of a $\{\mathbf{Pd}_{84}\}$ ring cluster that has the same magic number as $\{\mathbf{Mn}_{84}\}$ but is assembled from a different range of building blocks and symmetry. This observation means we may consider the $\{\mathbf{Pd}_{84}\}$ ring as a molecular Rosetta Stone for us to decode the symmetry building block correlation present in all these cluster systems. In this way it appears possible to predict the assembly of nanoscale architectures, based on an established minimal building block set, symmetry number, and suggesting some cluster nuclearity magic numbers. As such, we predict the fivefold system $\{\mathbf{Pd}_{12}\}_5 \equiv \{\mathbf{Pd}_{60}\}$ that we postulate could have a "fullerene-like" ball structure (19). This proposal is also consistent with the classic example of $\{\mathbf{Mo}_{132}\} \equiv \{\mathbf{Mo}_{22}\}_6$-ball (7), which has a shape of sphere, rather than ring. The anticipated obstacle in crystallizing $\{\mathbf{Pd}_{60}\}$ would be its assumed high solubility by virtue of the cluster's hydrophilic surfaces, but may be overcome by increasing the concentration of electrolyte in the solution in future. Preliminary MS studies show a mixture of highly charged species in the solution, and one peak at $m/z = 1{,}515.0$ can be assigned to the characteristic formula $[(\mathrm{Pd_5O_5})_{12}(\mathrm{PO_4})_{30}\mathrm{H_{35}Na_{47}(H_2O)_{45}}]^{8-}$ implying the first experimental hint that this cluster does exist (see *SI Appendix*, Fig. S10).

Methods and Materials

Synthesis of Pd-Ring $\{\mathbf{Pd}_{84}\}$. $\mathrm{NaH_2PO_4}$-$\mathrm{Na_2HPO_4}$ solution (22 mL, 0.15 M) at a pH of 6.5–7.1 was added to $\mathrm{Pd(OAc)_2}$ (0.56 g, 2.5 mmol). The suspension was left stirring rigorously for 20 h. The dark red solution was centrifuged and filtered to remove a small amount of solids. The pH of the filtrate was checked, and a few drops of 1 M NaOH were added to adjust the pH to 4.5. Evaporation of the filtrate from an open beaker led to long well-formed reddish acicular crystals after a few days. The crystals were collected by filtration and air dried. Yield: ca. 15–20% (based on Pd). It is worth noting that a large variety of possible conditions were explored but these mostly resulted in the formation of the well-known smaller $\{\mathbf{Pd}_{15}\}$ and $\{\mathbf{Pd}_{17}\}$ cluster archetypes.

X-ray Diffraction Structure Analysis and Crystallographic Data. $\mathrm{Na_{56}H_{14}[Pd_{84}O_{42}(OAc)_{28}(PO_4)_{42}]\cdot 200H_2O}$, $\mathrm{C_{56}H_{498}Na_{56}O_{466}P_{42}Pd_{84}}$, Mr $= 20156.33$; block crystal: $0.18 \times 0.12 \times 0.04$ mm^3; monoclinic, space group $P2_1/n$, $a = 14.7168(6)$, $b = 50.605(3)$, $c = 44.860(3)$Å, $\beta = 95.018(3)^\circ$, $V = 33{,}281(3)$Å^3, $Z = 2$, $\rho = 2.011$ gcm^{-3}, $\mu(\mathrm{Mo}_{\mathrm{K}\alpha}) = 2.44$ mm^{-1}, $F(000) = 19{,}344$; 260,069 reflections measured, 65,281 unique ($R_{\mathrm{int}} = 0.104$), 2,629 refined parameters, $R_1 = 0.0705$ $wR_2 = 0.2116$. Crystal data were measured on a Bruker Apex II Quazar diffractometer using $\mathrm{Mo}_{\mathrm{K}\alpha}$ radiation ($\lambda = 0.71073$ Å) at 150(2) K. Structure solution and refinement was carried out using SHELXL-97 and WinGX via a full matrix least-squares on F^2 method. All nonhydrogen atoms were refined anisotropically unless otherwise stated. This data can be obtained free of charge from Cambridge Structural Database for compound $\{\mathbf{Pd}_{84}\}$ from Cambridge Crystallographic Data Centre (CCDC), Cambridge, UK; e-mail deposit@ccdc.cam.ac.uk, CCDC 846615.

ACKNOWLEDGMENTS. F.X. thanks the Chinese Scholarship Council. We thank Mr Andrew Macdonell for help with the graphical representation of $\{\mathbf{Pd}_{60}\}$ and the associated animations. This work was supported by the Engineering and Physical Sciences Research Council (UK). L.C. thanks the Royal Society/Wolfson Foundation for a Merit Award.

1. Cronin L, et al. (2010) Unveiling the transient template in the self-assembly of a molecular oxide nanowheel. *Science* 327:72–74.
2. Philp D, Stoddart JF (1996) Self assembly in natural and unnatural systems. *Angew Chem Int Ed* 35:1155–1196.
3. Müller A, Bekmann E, Bögge H, Schmidtmann M, Dress A (2002) Inorganic chemistry goes protein size: A $\mathrm{Mo_{368}}$ nano-hedgehog initiating nanochemistry by symmetry breaking. *Angew Chem Int Ed* 41:1162–1167.
4. Whitesides GM, Grzybowski B (2002) Self-assembly at all scales. *Science* 295:2418–2421.
5. Kitagawa S, Kitaura R, Noro SI (2004) Functional porous coordination polymers. *Angew. Chem. Int. Ed* 43:2334–2375.
6. Teo BK, Sloane NJA (1985) Magic numbers in polygonal and polyhedral clusters. *Inorg Chem* 24:4545–4558.
7. Müller A, Krickemeyer E, Bögge H, Schmidtmann M, Peters F (1998) Organizational forms of matter: An inorganic super fullerene and Keplerate based on molybdenum oxide. *Angew Chem Int Ed* 37:3360–3363.
8. Tasiopoulos AJ, Vinslava A, Wernsdorfer W, Abboud KA, Christou G (2004) Giant single-molecule magnets: A $\{\mathrm{Mn_{84}}\}$ torus and its supramolecular nanotubes. *Angew Chem Int Ed* 43:2117–2121.
9. Müller A, et al. (1998) Formation of a ring-shaped reduced "metal oxide" with the simple composition $[(\mathrm{MoO_3})_{176}(\mathrm{H_2O})_{80}\mathrm{H_{32}}]$. *Angew Chem Int Ed* 37:1220–1223.
10. Müller A, et al. (1995) $[\mathrm{Mo_{154}(NO)_{14}O_{420}(OH)_{28}(H_2O)_{70}}]^{(25\pm5)-}$: A water-soluble big wheel with more than 700 atoms and a relative molecular mass of about 24000. *Angew Chem Int Ed* 34:2122–2123.
11. Takeda N, Umemoto K, Yamaguchi K, Fujita MA (1999) Nanometre-sized hexahedral coordination capsule assembled from 24 components. *Nature* 398:794–796.
12. Fujita M, Tominaga M, Hori A, Therrien B (2005) Coordination assemblies from a Pd(II)-cornered square complex. *Acc Chem Res* 38:369–378.
13. Kortz U, et al. (2008) Self-assembly of a heteropolyoxopalladate nanocube: $[\mathrm{Pd^{II}}_{13}\mathrm{As^{V}}_8\mathrm{O_{34}(OH)_6}]^{8-}$. *Angew Chem Int Ed* 47:9542–9546.
14. Cronin L, et al. (2011) A supramolecular heteropolyoxopalladate $\{\mathrm{Pd_{15}}\}$ cluster host encapsulating a $\{\mathrm{Pd_2}\}$ dinuclear guest: $[\mathrm{Pd^{II}}_2 \subset \{\mathrm{H_7Pd^{II}}_{15}\mathrm{O_{10}(PO_4)_{10}}\}]^{9-}$. *J Am Chem Soc* 133:4684–4686.
15. Zhang Y, Puddephatt RJ, Manojlović-Muir L, Muir KW (1996) First complex containing a $\mathrm{Pd_4}(\mu_4\text{-O})$ functional group. *Chem Commun* 22:2599–2600.
16. Hosokawa T, Takano M, Murahashi SI (1996) The first isolation and characterization of a palladium-copper heterometallic complex bearing μ_4-oxo atom derived from molecular oxygen. *J Am Chem Soc* 118:3990–3991.
17. Sharp PR (2000) Oxo and imido ligands in late transition metal chemistry. *J Chem Soc Dalton Trans* 16:2647–2657.
18. Kong XJ, Long LS, Zheng Z, Huang RB, Zheng LS (2010) Keeping the ball rolling: Fullerene-like molecular clusters. *Acc Chem Res* 43:201–209.
19. Brockman JT, Stamatatos TC, Wernsdorfer W, Abboud KA (2007) Synthesis and characterisation of a $\mathrm{Mn_{22}}$ single-molecular magnet and a $[\mathrm{Mn_{22}}]_n$ single-chain magnet. *Inorg Chem* 46:9160–9171.